Wegner, A. (1982b) *J. Mol. Biol. 161*, 607-615.
Wegner, A., & Savko, P. (1982) *Biochemistry 21*, 1909-1913.
Wegner, A., & Isenberg, G. (1983) *Proc. Natl. Acad. Sci. U.S.A. 80*, 4922-4925.
Wegner, A., Schröer, E., Selve, N., & Ruhnau, K. (1987) *Fortschr. Zool. 34*, 77-85.
Woodrum, D. T., Rich, S. A., & Pollard, T. D. (1975) *J. Cell Biol. 67*, 231-237.
Yang, Y. Z., Korn, E. D., & Eisenberg, E. (1979) *J. Biol. Chem. 254*, 7137-7140.
Yin, H. L., & Stossel, T. P. (1979) *Nature (London) 281*, 583-586.

Comparison of the Structure and Dynamics of Chicken Gizzard and Rabbit Cardiac Tropomyosins: ^{1}H NMR Spectroscopy and Measurement of Amide Hydrogen Exchange Rates†

Clive Sanders, Brian D. Sykes,* and Lawrence B. Smillie
MRC Group in Protein Structure and Function, Department of Biochemistry, University of Alberta, Edmonton, Alberta, Canada T6G 2H7

Received January 28, 1988; Revised Manuscript Received May 6, 1988

ABSTRACT: The side chain and backbone mobilities of chicken gizzard tropomyosin (TM) and its nonpolymerizable derivative have been investigated by ^{1}H NMR spectroscopy and amide hydrogen exchange kinetics and compared to those of rabbit cardiac TM and its nonpolymerizable derivative. Analysis of the 300-MHz ^{1}H NMR spectra of native chicken gizzard and rabbit cardiac TMs and their nonpolymerizable derivatives showed that the line widths of the aromatic and histidine residues were within a factor of 2 for all four proteins, demonstrating that the side chain mobility of these residues is similar in the different TMs. Direct proton exchange-out kinetics were determined in D_2O in the pD range 1.5-3.0 at 25 °C by ^{1}H NMR spectroscopy. Multiple exponential fitting of the exchange data indicated the presence in gizzard TM of at least three kinetically distinct classes of amide hydrogens at pD 1.7 with average population sizes of 147, 74, and 61, whose rates were retarded by a factor of 10, 10^3, and 10^5, respectively, relative to the random-coil peptide poly(DL-alanine). Measurement of the direct exchange kinetics of both rabbit cardiac and nonpolymerizable gizzard TMs showed that their rate constants and population sizes were within experimental error of those for the gizzard protein, except that the fast exchanging class for cardiac TM was increased in size while that of the nonpolymerizable gizzard TM was reduced, relative to that for gizzard TM. Comparison of the exchange-out kinetics for the cardiac and gizzard proteins at pH 2.0 and 55 °C, where only the two slowly exchanging amide hydrogen sets are measured, again demonstrated the similarity of their kinetic parameters. Amide hydrogen exchange in the pH range 6-11 was studied by NMR measurement of the transfer of saturation from water to the amide hydrogens. The loss in amide hydrogen intensity of the nonpolymerizable forms of the gizzard and cardiac TMs paralleled each other and was modeled using the kinetic parameters derived at acidic pH for the gizzard protein. The retardation factors for the fast and intermediate classes of amide hydrogens were decreased at the higher pHs so that they were only 2-fold and 10-fold, respectively, slower than the rate for the random-coil polypeptide. Differential scanning calorimetry of gizzard TM and its nonpolymerizable derivative indicated the presence of domains of differing thermal stability in both proteins at acidic and alkaline pH. The thermal unfolding properties of the two gizzard proteins were very similar to each other, both being considerably more stable at pH 2.0 than at pH 7.0, an observation which has been previously made with rabbit skeletal TM. Circular dichroism measurements on the variation of the α-helical content with temperature of gizzard TM and its nonpolymerizable derivative at pH 2.0 and 7.0 also showed that the two proteins' structures were of comparable stability. We conclude from these results that the relative mobility and stability of the gizzard and cardiac proteins are very similar and that whereas 20% of each molecule is in a relatively immobile and stable conformation, over half is in a more mobile, less stable conformation.

Tropomyosin (TM)[1] is of central importance in the regulation of contraction in muscle and cellular motile systems [see Smillie (1979); Talbot and Hodges (1982); Côté (1983); Leavis and Gergely (1984); and Payne and Rudnick (1985)]. The function of TM is best understood in striated muscle, where it serves to propagate conformational changes which start in the troponin complex (in response to changes in [Ca^{2+}]) to actin and thereby regulate the actomyosin ATPase. The structural features of TM responsible for its interaction with actin and the members of the troponin complex have been investigated as have those responsible for the stabilization of its coiled-coil structure and heat to tail overlap [for a review, see Leavis and Gergely (1984)]. In comparison, the role of TM in smooth muscle is more obscure. Here, contraction is

† Supported by the Medical Research Council of Canada.

[1] Abbreviations: TM, tropomyosin; NPTM, nonpolymerizable tropomyosin; DSS, disodium 2,2-dimethyl-2-silapentane-5-sulfonate; PDLA, poly(DL-alanine); NMR, nuclear magnetic resonance.

0006-2960/88/0427-7000$01.50/0

thought to be primarily controlled by the Ca^{2+}-dependent phosphorylation of the myosin light chains (Small & Sobieszek, 1980; Walsh et al., 1983; Adelstein & Eisenberg, 1980) and not by a troponin-like protein complex which several investigations have failed to demonstrate. However, recent studies have shown that smooth muscle TM has a modulatory role on actomyosin ATPase activity in vitro (Sobieszek, 1982; Hartshorne et al., 1977; Lehrer & Morris, 1984; Williams et al., 1984), potentiating this activity under most but not all conditions, in contrast to the inhibitory effect of skeletal muscle TM. These effects have been interpreted by Williams et al. (1984) and Lehrer and Morris (1984) in terms of the allosteric model of Hill et al. (1980): more of the TM–actin complex is in the "strong S-1-binding form" with smooth muscle TM than with skeletal TM.

To further our understanding of the underlying structural features of gizzard TM responsible for its differing functional properties, we undertook the elucidation of the amino acid sequences of its two major isoforms, β and γ (Lau et al., 1985; Sanders & Smillie, 1985; Helfmann et al., 1984). These isoforms, which together constitute the native heterodimer (Sanders et al., 1986), have the same polypeptide chain length (284 residues) as their skeletal counterparts. Further, as is expected from the known gene organization of TM (MacLeod, 1987; Ruiz-Opazo & Nadal-Ginard, 1987), both are highly homologous to the rabbit skeletal proteins apart from the regions of residues 43–80 in γTM, residues 189–213 in βTM, and residues 258–284 in both isoforms. The observed interaction properties of gizzard TM have been correlated (Sanders & Smillie, 1985) to some of these structural elements. Thus, the altered COOH-terminal sequences lead to a strengthening of its head to tail polymerization and a weakening of its binding to troponin, whereas its binding to actin is similar to that of rabbit skeletal TM as is expected from the high degree of homology between the two proteins (Sanders & Smillie, 1984).

In a recent report (Sanders et al., 1986), we discussed the proposition that gizzard TM is a more rigid (Lehrer et al., 1984) molecule than its skeletal counterpart. We concluded that, while the analyses of the putative ionic g to e interactions of the sequences would suggest that, if anything, the stability of the gizzard TM molecule would be less than rabbit skeletal $\alpha\alpha$TM, there was inadequate evidence to assess the relative flexibilities of these proteins. In the present report, we have investigated this question by an analysis of the NMR spectra of their aromatic amino acids, which gives information on side chain dynamics (Edwards & Sykes, 1977), and by studying their amide hydrogen exchange characteristics, which can provide detailed information on structural fluctuations in the polypeptide backbone [for a review, see Englander and Kallenbach (1984)].

Experimental Procedures

Preparation of Proteins. Chicken gizzard and rabbit cardiac tropomyosins were prepared as described by Smillie (1982) with a final ion-exchange chromatographic step for both proteins: hydroxyapatite for the cardiac and DEAE-cellulose for the gizzard. Cardiac TM was dephosphorylated with diisopropyl fluorophosphate treated *Escherichia coli* alkaline phosphatase (Cooper Biomedicals Ltd., Westchester, PA) at a molar ratio of enzyme to substrate of 1:100 in 150 mM NaCl, 10 mM $MgCl_2$, and 50 mM Tris-HCl, pH 8.0, for 3 h at 37 °C. This preparation or its carboxypeptidase-treated derivative was used in all experiments. The nonpolymerizable forms of both smooth and striated TMs were prepared as described by Heeley et al. (1987). The extent of the diisopropyl fluorophosphate treated carboxypeptidase A (Sigma) digestion was monitored by amino acid analysis; several analyses indicated that 36 amino acids were released per mole of gizzard TM; i.e., the digestion was essentially quantitative and stopped at the Glu-Glu sequence of residues 265–266. Similarly, the digestion of cardiac protein was arrested at residue 273.

Ultracentrifugation Studies. Sedimentation studies were done at 20 °C on a Beckman Model E analytical ultracentrifuge equipped with a photoelectron scanner, a multiplex accessory, and a high-intensity light source. Low-speed sedimentation equilibria runs were performed according to Chervenka (1969) at 10000 rpm for cardiac TM and at 7200 rpm for the gizzard protein.

Differential Scanning Calorimetry. Thermal unfolding studies of TM were done in an MC-2 high-sensitivity scanning calorimeter (Microcal, Inc., Amherst, MA). Protein samples were reduced with 20 mM DTT at pH 8.0 prior to dialysis to final buffer conditions. Heat capacity profiles presented under Results were selected from a minimum of three DSC runs for that sample.

Circular Dichroism. Spectra were recorded on a Jasco J-500c spectropolarimeter attached to a Jasco J-500N data processor. The sample compartment was water jacketed and heated with a Lauda thermoregulator. Sample temperature values were determined from a calibration run with buffer in which in temperature of the sample compartment was related to that of the circulating water. The instrument was routinely calibrated with an aqueous solution of recrystallized *d*-camphorsulfonic acid. Protein was reduced with 20 mM DTT at pH 8.5 prior to dialysis to final buffer conditions. Protein concentrations were in the range 0.2–0.5 mg/mL.

^1H Nuclear Magnetic Resonance Spectra of Fully Exchanged TMs. Samples were dissolved in 1 M KCl, 1 mM EDTA, 10 mM DTT, and 40 mM phosphate, pH 7.0, and dialyzed against this buffer overnight at 4 °C; their concentrations were determined by amino acid analysis and adjusted to give 3.3 mg/mL (0.05 mM). The samples were then fully exchanged with D_2O by repeated lyophilization and dissolved in the appropriate volume of D_2O (0.7 mL), and their spectra were recorded, after which their protein concentration was again determined by amino acid analysis. ^1H NMR spectra was recorded on a Nicolet NT-300WB spectrometer operating at 300 MHz in the Fourier-transform mode. Instrument settings were as follows: number of transients, 50000; pulse width, 70°; acquisition time, 1.0 s; sweep width, 4000 Hz; spectrum size, 8192 data points collected in the double precision mode; 2-Hz line broadening. The HDO resonance was reduced with homonuclear decoupling. All chemical shifts are referenced to the major resonance of DSS.

Kinetic Measurements of Hydrogen Exchange. Protein samples were initially dissolved in 30 mM phosphate buffer, pH 8.5, at a protein concentration of 0.25 mM and reduced with 20 mM DTT for 1 h at room temperature. This was followed by dialysis overnight at 4 °C to final buffer conditions: 60 mM phosphate 10–20 mM HCl, pH 1.7–3.7, and lyophilization of 0.600-μL volumes. Proton efflux was initiated by dissolving the freeze-dried powder in 600 μL of D_2O. ^1H NMR spectra, at 300 MHz, of TM solutions in 5-mm NMR tubes were recorded with a Nicolet NT 300WB NMR spectrometer with the following parameters: acquisition time, 1 s; sweep width, 8000 Hz; spectrum size, 16384 data points; pulse width, 7 μs (70°); 2-Hz line broadening. Usually 400–600 transients (6.6–10.2 min) were acquired. The symbol pD is used to indicate the pH was measured for D_2O solutions. No correction to the meter reading was made, since the deu-

terium isotope effect on the glass electrode and the pK_a's of typical acids are approximately compensating (Bundi & Wuthrich, 1979).

Steady-State NMR Measurements of Hydrogen Exchange. A measure of hydrogen exchange rates is also afforded by measuring the transfer of saturation from the water resonance to that of the amide by exchange (Forsen & Hofmann, 1964; O'Neil & Sykes, 1988). When the exchange rate is of the order of or faster than the spin–lattice relaxation rate of the amide proton ($1/T_{1NH}$), the fractional amide intensity (M_Z/M_Z^0) will be reduced to $1/(1 + k_{ex}T_{1NH})$ due to saturation transfer. In these experiments, samples were reduced in 30 mM DTT–50 mM phosphate, pH 8.0, for 1 h prior to dialysis overnight to final buffer conditions: 1 M KCl, 1 mM EDTA, 10 mM DTT, and 10 mM KH_2PO_4, pH 6.2. The proteins were then lyophilized, followed by dissolution in 80% H_2O–20% D_2O. Instrument settings were the following: water preirradiation, 1.5 s; pulse width, 7 μs (70°); number of acquisitions 6000; acquisition time, 0.8 s; sweep width, 10 000 Hz; 8192 data points collected in the double precision mode. The nonpolymerizable TM solutions were titrated to the appropriate pH with 1 M NaOH.

RESULTS

^{1}H NMR Spectroscopy of Gizzard and Cardiac TMs and Their Nonpolymerizable Derivatives. Previous work from this group was assigned and characterized the histidine ^{1}H NMR resonances of rabbit striated muscle TM and reported on their sensitivity to the conformational state of the molecule (Edwards & Sykes, 1978, 1980). In addition, the NMR spectra of the tyrosine and phenylalanine residues have been analyzed in comparison to those calculated for a tyrosine residue, with varying degrees of internal rotational diffusion, placed on an idealized α-helical rod (Edwards & Sykes, 1977), with the conclusion that the aromatic residues were not fixed rigidly in the coiled-coil structure but did exhibit side chain mobility.

Figure 1 shows the aromatic portion of the ^{1}H NMR spectra of both gizzard and cardiac TMs and their nonpolymerizable derivatives. On the basis of the work of Edwards and Sykes (1977), the assignments for the aromatic portion of NMR spectra of rabbit cardiac TM as shown in Figure 1 are as follows: δ 6.8, tyrosine 3,5 protons (24); δ 7.3, histidine C4 protons (4); δ 7.1–7.5, tyrosine 2,6 protons (24) and phenylalanine protons (10); δ 8.1, C2 protons of histidine 153 (2); δ 8.2, C2 protons of histidine 276 (2); δ 8.5, formate ion. Similar assignments can be made for gizzard TM with the broad peak at 8.1–8.4 ppm arising from histidine-153 and 271 C2 proton resonances which are on both chains of the $\beta\gamma$ heterodimer and from the single γ-chain histidine-65 C2 proton resonance. Comparison of the spectra in Figure 1 is complicated by the tyrosine content of the two proteins (gizzard TM has 7 residues per 66 000-dalton molecule, whereas cardiac has 12) and by their histidine content (gizzard TM has 5 compared to cardiac's 4). Both nonpolymerizable TMs have the same tyrosine content as their parent molecules but histidines-271 and -276 have been removed from the gizzard and skeletal proteins by carboxypeptidase A treatment.

Interpretation of the NMR spectra of TM is further complicated by its ability to form head to tail aggregates which have longer correlation times and consequently broader spectra. Therefore, to facilitate an analysis of the relative flexibility of gizzard and cardiac TMs, it is necessary to ensure that their polymerization states are comparable. To accomplish this, the NMR experiments shown in Figure 1 were carried out at low protein concentration (3.6–3.9 mg/mL) and high ionic strength (1 M KCl–40 mM phosphate, pH 7.0). Sedimentation

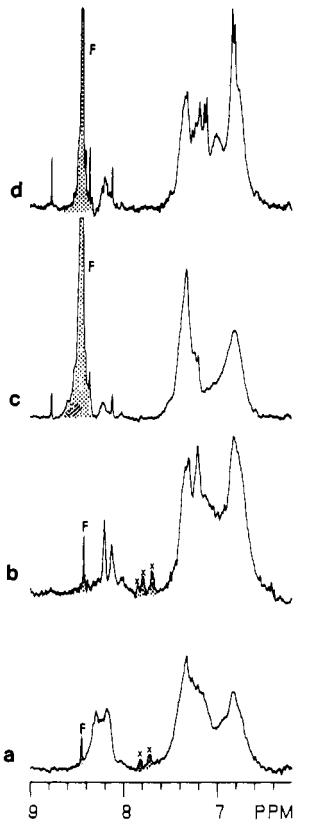

FIGURE 1: Aromatic portions of the 300-MHz ^{1}H NMR spectra of gizzard and cardiac TMs at 25 °C and pH 7.0 in 1 M KCl, 10 mM DTT, and 40 mM phosphate. (a) Native chicken gizzard TM, 3.9 mg/mL; (b) native rabbit cardiac TM, 3.6 mg/mL; (c) nonpolymerizable gizzard TM, 3.9 mg/mL; (d) nonpolymerizable cardiac TM, 3.6 mg/mL. The shaded portions of the spectra marked with formate ion (F) or X represent small molecule impurities.

equilibrium studies under these conditions gave molecular weights of about 64 000 for both TMs and their nonpolymerizable derivatives. However, the presence of minor higher molecular weight species (up to M_r of 100 000) was detected in the polymerizable TM solutions, indicating an equilibrium monomers and dimers which largely favors the former species.

Examination of the results presented in Figure 1, with the above considerations noted, allows an assessment of the relative rotational mobility of the aromatic side chains of the proteins by inspection of their respective line widths. Two observations are apparent. First, the spectra of the nonpolymerizable TMs are very similar to those of their parent molecules. Thus, removal of 22 and 36 amino acids from the C-termini of rabbit cardiac and chicken gizzard TMs, respectively, does not lead to a dramatic change in the relative mobility of the remaining residues, implying that the conformation of the protein in the vicinity of the removed residues is unaltered. However, it is also apparent that the carboxypeptidase A treatment of cardiac TM results in the appearance of two sharp doublets at δ 6.8 and δ 7.1, the characteristic chemical shift values for the 3,5 and 2,6 protons of tyrosine residues in linear peptides (Bundi & Wuthrich, 1979). The most likely assignment for these resonances is to tyrosine-267 which is only six residues away from the C-terminus in the nonpolymerizable form and so might experience greater mobility. Further support for this assignment comes from the fact that it is not seen in the spectrum of the gizzard TM which does not have tyrosine in this position.

The second observation is that the line widths of the aromatic resonances (focusing, for example, on the resonance

Table I: Multiple Exponential Least-Squares Fits of Proton Exchange Data as a Function of pH[a]

pD	k_{ex_1} (min^{-1})	n_1	k_{ex_2} (min^{-1})	n_2	k_{ex_3} (min^{-1})	n_3	$\sum_i n_i$
1.66	$(3.5 \pm 0.26) \times 10^{-2}$	151 ± 4	$(6.2 \pm 1.1) \times 10^{-4}$	75 ± 5	$(7.6 \pm 2.1) \times 10^{-6}$	58 ± 5	284 ± 14
1.90	$(2.8 \pm 0.19) \times 10^{-2}$	128 ± 4	$(3.7 \pm 0.6) \times 10^{-4}$	102 ± 7	$(7.6 \pm 3.1) \times 10^{-6}$	56 ± 8	286 ± 19
1.93	$(6.0 \pm 0.96) \times 10^{-2}$	129 ± 7	$(15.3 \pm 3.8) \times 10^{-4}$	74 ± 6	$(17.7 \pm 2.6) \times 10^{-6}$	80 ± 5	283 ± 18
2.06	$(2.3 \pm 0.18) \times 10^{-2}$	156 ± 8	$(6.9 \pm 1.2) \times 10^{-4}$	63 ± 3	$(9.2 \pm 2.0) \times 10^{-6}$	55 ± 3	274 ± 14
2.07	$(3.1 \pm 0.13) \times 10^{-2}$	151 ± 3	$(9.2 \pm 1.6) \times 10^{-4}$	56 ± 3	$(13.3 \pm 1.4) \times 10^{-6}$	75 ± 3	282 ± 9
2.77	$(10.5 \pm 1.49) \times 10^{-2}$	157 ± 7	$(54.8 \pm 8.5) \times 10^{-4}$	71 ± 5	$(33.1 \pm 5.9) \times 10^{-6}$	55 ± 3	283 ± 15
2.93	$(7.0 \pm 0.59) \times 10^{-2}$	159 ± 6	$(8.0 \pm 1.6) \times 10^{-4}$	74 ± 4	$(14.3 + 3.2) \times 10^{-6}$	50 ± 4	283 ± 14
1.93[b]	$(8.5 \pm 1.0) \times 10^{-2}$	129 ± 6	$(14.3 \pm 3.3) \times 10^{-4}$	60 ± 4	$(11.9 \pm 1.7) \times 10^{-6}$	75 ± 3	264 ± 13
2.00[c]	$(4.5 \pm 0.1) \times 10^{-2}$	176 ± 2	$(7.8 \pm 1.1) \times 10^{-4}$	57 ± 4	$(21.8 \pm 4.4) \times 10^{-6}$	49 ± 5	282 ± 11
2.00[d]	$(1.16 \pm 0.08) \times 10^{-2}$	50 ± 1	$(1.6 \pm 0.2) \times 10^{-4}$	39 ± 1			89 ± 2
2.00[c,d]	$(1.06 \pm 0.01) \times 10^{-2}$	56 ± 3	$(1.8 \pm 0.6) \times 10^{-4}$	47 ± 2			103 ± 5

[a] k_{ex_i} (i = 1, 2, 3) are the first-order rate constants; n_i are the number of amides exchanging at a particular rate. The errors were determined from the standard deviations of the fits. Data sets are for gizzard TM except where indicated. [b] Nonpolymerizable gizzard TM. [c] Rabbit cardiac TM. [d] Data obtained at 55 °C and fitted to two exponentials. All other data obtained at 25 °C.

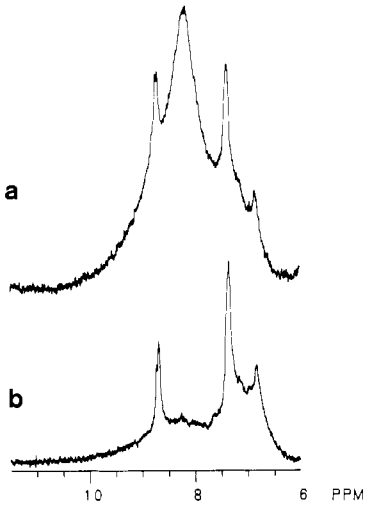

FIGURE 2: Aromatic and amide regions of the 300-MHz ^{1}H NMR spectrum of gizzard TM at 25 °C and pD 2.11 17 min (a) and 25 days (b) after dissolution in D_2O at a protein concentration of 0.25 mM (16.5 mg/mL).

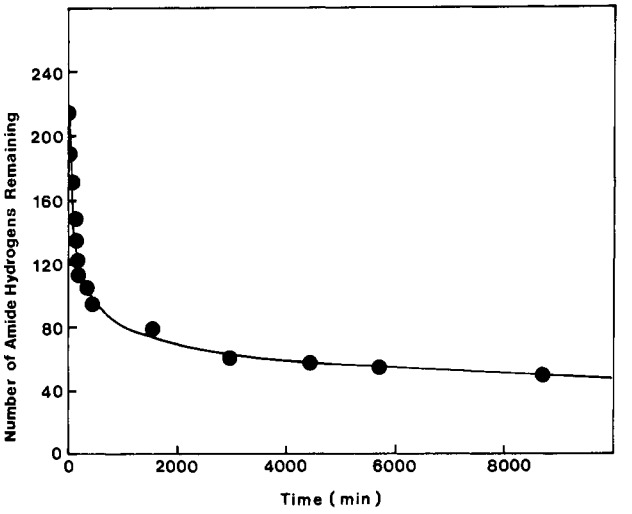

FIGURE 3: Amide hydrogen decay curve of gizzard TM at 25 °C in 10 mM phosphate, pD 2.11, at a protein concentration of 0.25 mM (16.5 mg/mL). For clarity, the later time points (up to 60 000 min) have been omitted.

centered at 6.8 ppm corresponding to the 3,5 protons of the tyrosines) are comparable within a factor of 2 for the cardiac and gizzard proteins. If anything, the line widths appear to be slightly broader for the gizzard protein, but this could be due to greater heterogeneity in the chemical shifts for the gizzard protein which is a heterodimer of two different chains.

In summary then, the NMR spectra of the four TMs, recorded under identical conditions, demonstrate that the relative mobilities of their aromatic residues, and therefore by implication their overall conformations, are of comparable magnitude.

^{1}H NMR Kinetic Measurements of Hydrogen Exchange. Figure 2a shows a representative ^{1}H NMR spectrum of the amide and aromatic region of gizzard TM at 17 min after dissolution of the protein in D_2O at low pD. The NMR spectrum consists of the relatively sharp resonances of the histidine and aromaic protons superimposed upon a broad set of resonances from the polypeptide amide hydrogens, centered at 8.2 ppm. The appearance of the spectrum after several days (Figure 2b) has not changed with the exception that the intensity of the amide proton peak has been reduced due to exchange with D_2O.

For the quantification of the number of protons present at a particular time, the spectrum was fitted to a number of theoretical curves generated by the Nicolet curve analysis program with the following restraints: (1) the ratio of the combined integrated intensity of the tyrosine + phenylalanine + histidine C4 protons to the integrated intensity of histidine C2 protons approached as closely as possible the ratio of the number of these protons in the protein; (2) the root mean square deviation between the experimental and modeled curve was the lowest possible value. The number of amide hydrogens was then calculated by comparison of the integrated intensity under the amide hydrogen peak to the average integrated intensity of histidine, tyrosine, and phenylalanine hydrogens. In initial calculations, this procedure was carried out on each time point in a series for a particular pD value. However, it was later found that comparable results were obtained by analyzing the last time point in a series in this manner, correlating the peak height for the amide proton resonance to the number present and then determining the number present at earlier times from peak heights since there was no change in line width throughout the reaction. Typical results for gizzard TM are shown in Figure 3.

Exchange rates for different pDs were then determined by fitting the results to $\sum_i A_i \exp(-k_{ex_i} t)$ (i = 1–4) with a nonlinear least-squares fitting routine. The time for each point was chosen as the midpoint of the acquisition period. Although the data fitted well to four exponentials, the best standard deviations of the kinetic parameters were given with a three-exponential fit, and these results are presented in Table I and Figure 4.

These results show that the amide hydrogens of gizzard TM can be separated into three kinetic classes, which differ in their rates by a factor of 10^2. The number of amide hydrogens present in these classes are given in Table I with average values of 147 ± 6, 76 ± 5, and 61 ± 4 (sum = 282 ± 15) for the

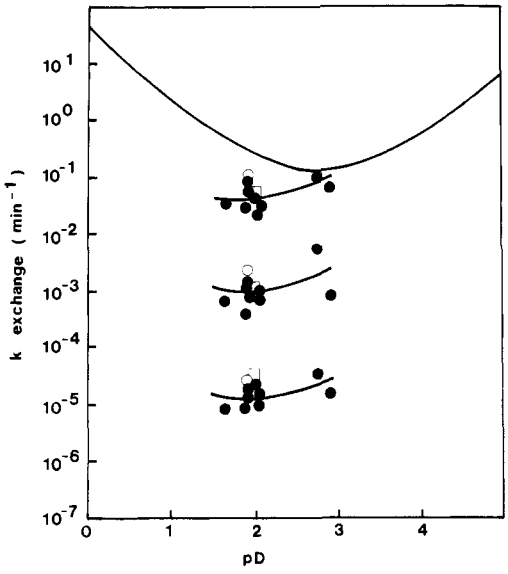

FIGURE 4: Plot of log k_{ex} vs pD from the data in Table I. The lines through the three sets of data are meant to guide the eye and are not least-squares fits. For comparison, the theoretical curve for the exchange of poly(DL-alanine) at 25 °C is shown. The equation for this curve is $k_{ex}^{25} = (6.419 \times 10^{8})10^{+pD-14.873} + 0.588 \times 10^{-pD}$ as described by O'Neil and Sykes (1988) and calculated from Roder et al. (1985). The points marked with (□) and (○) are for cardiac TM and nonpolymerizable gizzard TM, respectively.

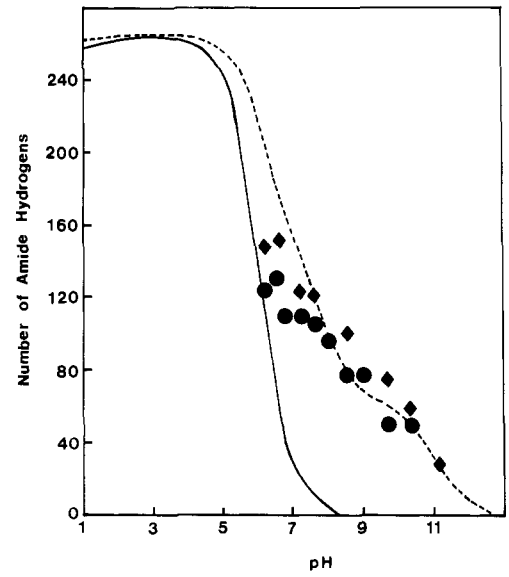

FIGURE 5: Plot of the pH dependence of amide proton resonance intensity for nonpolymerizable gizzard (♦) and cardiac TMs (●) acquired in 80% H_2O–20% D_2O at 25 °C with presaturation of the solvent. Protein concentration was 0.25 mM in 1 M KCl, 1 mM EDTA, 10 mM DTT, and 10 mM phosphate. The solid line depicts the predicted loss in amide intensity for a hypothetical 266-residue random-coil poly(DL-alanine) at 25 °C. The dashed line shows the predicted loss in amide intensity for another hypothetical 266-residue polypeptide divided into sets of amide hydrogens of size 130, 74, and 61 which have exchange rates retarded by factors of 2, 5, and 10^5 relative to the random-coil poly(DL-alanine). The equations used for these models are taken from the legend for Figure 4 with the appropriate retardation factors applied.

fastest to slowest group, respectively, in gizzard TM. Also shown in Figure 4 is a theoretical curve for the pD dependence of exchange in PDLA, constructed by using the equations of Roder et al. (1985) as described by O'Neil and Sykes (1988). Comparison of this curve with the results for gizzard protein indicates that the three sets of amide hydrogens are retarded approximately by 1, 3, and 5 decades at pD 2.0 and 25 °C relative to PDLA. Exchange-out experiments were also performed on rabbit cardiac and nonpolymerizable gizzard TMs, and these results are given in Table I and also plotted in Figure 4. The rate constants for both proteins are within experimental error for those for the gizzard TM. The population sizes are also similar, except that whereas the fast exchanging class of the nonpolymerizable TM is reduced relative to gizzard TM, perhaps due to the removal of 18 residues from its C-terminus, that for the striated muscle protein has increased, with the possible implication that this loosely structured region is more extensive in this molecule. Of course, verification of this interpretation requires more extensive experimentation.

The exchange characteristics of the smooth and striated muscle proteins were also studied at 55 °C, pD 2.0, analyzed as before, and found to fit best to two exponentials. The results are presented in Table I. The two classes discernible at this temperature presumably correspond to the slower ones identified at 25 °C, with their rates increased in response to the higher temperature, the fast class exchanging out before they can be measured. Again, in agreement with the low-temperature studies, the kinetic parameters of the two proteins are closely matched, although the population sizes for the gizzard protein are slightly lower than those determined at 25 °C.

Steady-State Measurements of Amide Hydrogen Exchange. Exchange-out experiments were only performed in the narrow pD range of 1.7–3.0. In the pH range 3.0–6.0, near the isoelectric point (4.6) of TM, the protein was found to aggregate, making reliable measurments of the kinetics difficult. Above this pH, direct monitoring of amide hydrogen exchange rates is restricted to those with half-lives greater than about 12 min (k_{ex} less than 0.06 min^{-1}) since this much time is needed for measurement of the first time point; this translates into exchange rates which are 4 decades or more slower than the rate for PDLA at pH 7.0. This indicates that only the most slowly exchanging class of TM's amides could be measured. In addition, the propensity of TM for head to tail aggregation in the neutral pH range complicates quantitative analysis of its NMR spectra due to the concomitant increase in its line widths.

To overcome these difficulties, we chose to measure the steady-state level of amide hydrogens in the nonpolymerizable forms of the smooth and striated TMs. The number of amide hydrogens present at a given pH was determined by use of the curve-fitting procedure discussed above with the sharp resonances of the histidine and aromatic residues at the highest pH value serving as internal standards.

The results are presented in Figure 5. The solid line indicates the calculated pH dependence of amide intensity in a saturation transfer experiment at 25 °C for a PDLA polypeptide 266 residues long, i.e., the same length as the nonpolymerizable gizzard TM, with an assumed T_{1NH} of 1 s. The observed amide intensities for the two TMs have a similar pH dependence which is markedly different from that for the random-coil polypeptide, especially at high pH values. This is consistent with the exchange rate of their amide hydrogens being retarded, relative to PDLA, in agreement with the direct exchange-out studies at low pH. This suggested that it may be possible to "model" these results on the basis of the average class sizes and rate constants found at the lower pH values. The dashed curve in Figure 5 represents our attempt at this; it shows the calculated pH dependence of a PDLA polypeptide, with the same length as before, but with amide hydrogen population sizes of 130, 74, and 61 (i.e., the average population sizes found for the gizzard TM with 18 hydrogens removed

from the fastest class since the model is for the nonpolymerizable form) whose exchange rates have been slowed by factors of 2, 10, and 10^5 relative to PDLA. In this model, we have increased arbitrarily the exchange rate of the fastest and intermediate sets by factors of 5 and 10, respectively. Although the fit is not exact, the model does serve as a reasonable approximation to the observed pH dependence of the amide hydrogen intensity for both TMs.

Thus, the equilibrium measurements of amide exchange in the pH range 6.0–11.0 both support and extend the conclusions drawn from the direct exchange-out experiments at acidic pH. The chicken gizzard and rabbit striated nonpolymerizable TM amide hydrogens exhibit a similar relationship between amide intensity and pH, demonstrating that their exchange rates are of comparable magnitude with the corollary that the two proteins' structural mobilities are also of comparable magnitude. Furthermore, this relationship can be approximated by using the class sizes obtained at the low pH values, suggesting that the gross structure of the smooth and striated TMs does not change from pH 2 to 7, but, importantly, in this model the exchange rates of the fast and intermediate sets of amide hydrogens are increased relative to those at pH 2.0, implying that these amides are in a more flexible conformation at pH values around neutrality.

Thermal Unfolding Properties. The stability of gizzard TM to heat denaturation was monitored by two techniques, differential scanning calorimetry and circular dichorism. The heat capacity profiles for gizzard TM and its nonpolymerizable counterpart at different pHs are given in Figure 6. It is apparent that pH has a marked effect on the proteins' stabilities. At pH 2.0, the heat capacity profile of the native gizzard TM (curve b) is observed to contain two prominent transitions with T_m values of 65 and 76 °C, with the presence of minor transitions in the range of 68–72 and 81–84 °C, whereas at pH 7.0 (curve d) all of these have collapsed into a single endotherm with a midpoint value of 43 °C. Two transitions are again evident at pH 7.5 (curve e) with T_m's of 46 and 50 °C, and these are more pronounced at pH 10.5 (curve f) but with lower midpoint temperature values of 37 and 42 °C. The differential scanning calorimetric profiles of nonpolymerizable gizzard TM closely resemble those of its parent molecule; at pH 2.0 (curve a), two endotherms with T_m's of 68 and 80 °C are discernible which coalesce into one broad peak with a midpoint temperature of 43 °C at neutral pH (curve c). These results demonstrate that gizzard TM is segmented into regions of differing thermal stability at pHs above and below neutrality; however, at pH 7.0, only a single endotherm can be detected. A rational explanation for these observations is that the gizzard protein retains its domain structure at neutral pH but their thermal stabilities are such that their endotherms extensively overlap one another or, alternatively, that unfolding of one of the segments of the molecule triggers the unfolding of the rest of the structure.

The melting curves for native and nonpolymerizable gizzard TM at pH 2.0 and 7.0 as measured by their relative α-helical content are given in Figure 7. Consistent with the heat capacity profiles, both TMs are more stable under acidic conditions as judged by the midpoints of their transistions; at pH 2.0, their transistions are 64 °C (native) and 63 °C (nonpolymerizable), while at pH 7.0 these are reduced to 40 and 39 °C, respectively. Thus, it is also evident that removal of the 18 C-terminal amino acids from the gizzard TM does not dramatically affect its thermal unfolding pattern. A similar observation has been noted with cardiac NPTM in this laboratory (Mak & Smillie, 1981). Unfortunately, the domain

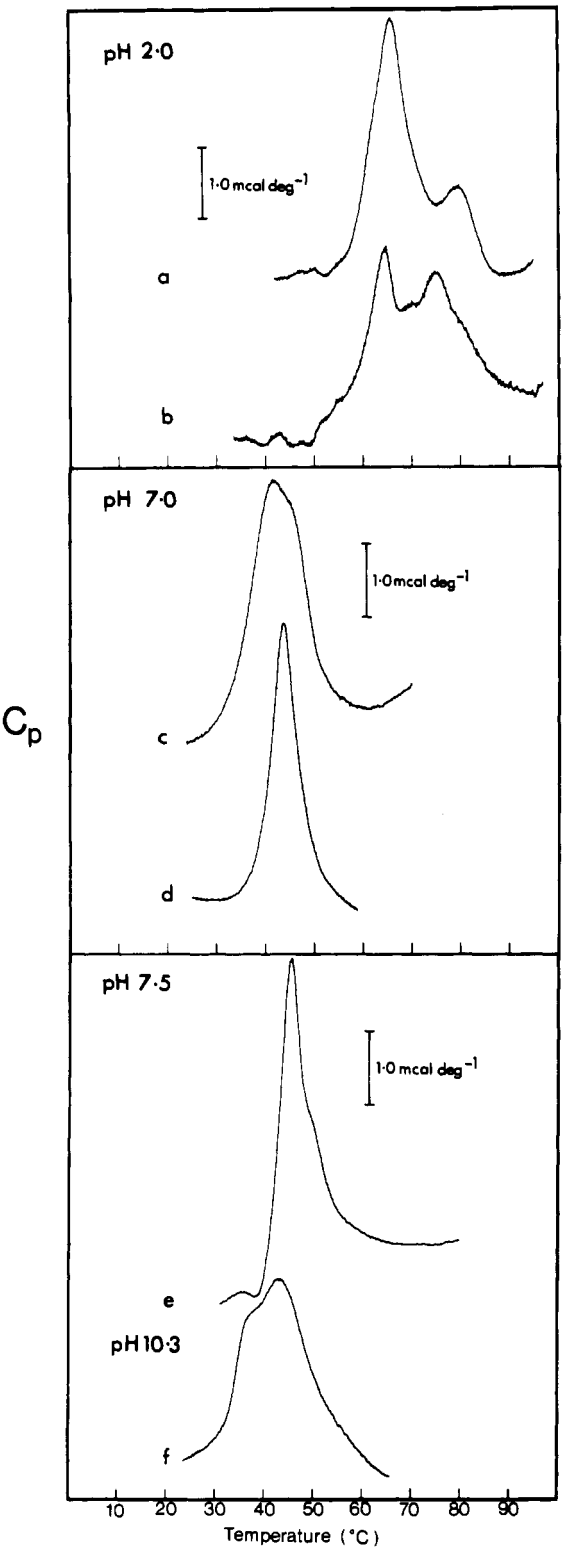

FIGURE 6: Heat capacity profiles of native and nonpolymerizable gizzard TM. (a) Nonpolymerizable gizzard TM (9.3 mg/mL); (b) native gizzard TM (10.0 mg/mL) at a relative scale factor of 1.5, in pH 2.0 10 mM phosphate–1 mM DTT; (c) nonpolymerizable gizzard TM (8.9 mg/mL); (d) native gizzard TM (9.2 mg/mL) at a relative scale factor of 0.5, in pH 7.0 0.1 M KCl, 10 mM phosphate, 1 mM DTT, and 1 mM EDTA; (e) 5.1 mg/mL gizzard TM in pH 7.5 10 mM phosphate, 1 M KCl, 1 mM EDTA, and 1 mM DTT; (f) 6.5 mg/mL gizzard TM in pH 10.3 10 mM phosphate, 1 M KCl, 1 mM EDTA, and 1 mM DTT. Sample size, 1.23 mL; scan rate, 45 °C/h.

structure of the smooth muscle protein is not readily apparent in these melting curves. This is most likely a consequence of the lack of sensitivity of this technique as compared to dif-

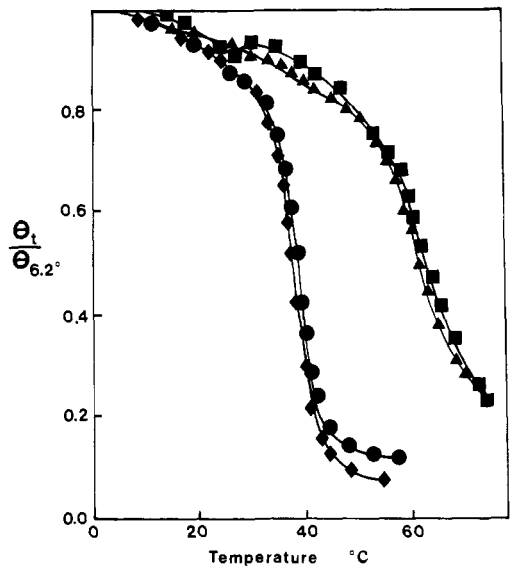

FIGURE 7: Thermal unfolding properties of gizzard TM and its nonpolymerizable derivative at pH 2.0 (▲ and ■, respectively) in 10 mM phosphate and at pH 7.0 (♦ and ●, respectively) in 10 mM phosphate, 0.1 M KCl, 10 mM DTT, and 1 mM EDTA, as determined by circular dichroism measurements. The α-helical content is calculated from the molar ellipticity at a particular temperature relative to that of TM at 6.2 °C.

ferential scanning calorimetry, where the derivative of the progress curve is measured.

Discussion

Relative Side Chain and Backbone Mobilities of Gizzard and Cardiac TMs. Lehrer et al. (1984) have reported that gizzard TM is a more rigid molecule than skeletal TM, whereas our analysis (Saunders et al., 1986) of the amino acid substitutions present in the smooth muscle protein indicated that their stabilities would be similar, with that of the gizzard molecule perhaps being slightly decreased. All of the evidence presented in this report demonstrates that these two protein structures are of comparable side chain and backbone mobilities and that, although regions of varying stability do exit in their strucures, these regions closely resemble one another in segment size and mobility. Thus, examination of the line widths of the proton resonances from the side chains of the tyrosine and histidine residues of the two TMs and their nonpolymerizable derivatives demonstrates that they all experience similar degrees of side chain mobility, and since the width of these resonances is considerably less than that calculated for a static residue (Edwards & Sykes, 1977) internal motion is indicated with resultant line narrowing. Further, the kinetic parameters derived from the direct exchange-out experiments on the smooth and striated TMs are virtually indistinguishable from one another. For instance, when the values obtained at pH 2.06 for gizzard TM are compared with those for cardiac TM at pH 2.00, they are all within experimental error of the fitting procedure, apart from the population size of the fastest class and exchange rate of the slowest class which are both slightly greater in magnitude for the cardiac protein.

To explore the backbone mobility of the gizzard and cardiac molecules at pH values around neutrality and above, we determined the amide hydrogen exchange as a function of pH for their nonpolymerizable derivatives from steady-state NMR methods. We chose to use the modified forms of the proteins so that interpretation of their spectra would not be complicated by the propensity of TM for head to tail aggregation. The use of these derivatives as models of their respective TMs is justified by the results from the circular dichroism and differential scanning calorimetry experiments which show that the structure of gizzard TM is not grossly altered by carboxypeptidase A treatment, a result that has been previously demonstrated in this laboratory for cardiac nonpolymerizable TM (Mak & Smillie, 1981). The relationship between pH and amide intensity is very similar for both molecules. Consistent with the direct exchange-out experiments at low pH, there appears to be more amide protons ($\cong$15) for gizzard TM in slow exchange throughout the high-pH region although the result is barley outside experimental error.

The results presented herein on the side chain mobility (^{1}H NMR spectroscopy) and backbone amide solvent accessibility (amide hydrogen exchange kinetics) of the gizzard and cardiac TMs do not support the contention that either molecule is markedly more restricted in its internal motion. However, that is not to say that the differences found in their amino acid sequences are not reflected in some way in their conformational parameters, which they undoubtedly are, but that these differences cause *subtle* changes in these structures. If anything, the aromatic side chain and backbone flexibilities appear less for the gizzard protein, but these conclusions are near the limits of the experimental error of the measurements.

Structural Stability of TM. The exchange-out kinetics at low pH were found to fit best to a linear combination of three exponentials. Laiken and Printz (1970) have shown that simulated hydrogen-exchange data composed of a random distribution of rate constants could be fitted well to only two or three distinct kinetic classes, raising doubts concerning the physical meaning of such data obtained for large macromolecules. Therefore, it is desirable to have independent evidence to confirm the existence of regions of varying stability in TM. The results from the differential scanning calorimetry experiments provide such confirmation. It is readily apparent in the heat capacity profiles of gizzard TM that domain structure is present in this molecule. These observations are in good agreement with those of Williams and Swenson (1981) for skeletal TM, whose heat capacity profiles contain two prominent and two minor transitions at pH 2.0 and 6.0 which collapse into two major transitions around neutrality and finally one transition at pH 8.0 for *N*-ethylmaleimide-treated TM. Indeed, Potekhin and Privalov (1982) in a separate study concluded from a deconvolution analysis of the heat capacity profiles for skeletal αTM that the molecule is composed of seven cooperative blocks. Optical rotary dispersion measurements on the stabilities of various TMs to heat and guanidinium chloride also support the idea that the unfolding of TM is a multistep process (Woods, 1976). The existence of domains in the structure of TM is therefore well established, and interpretation of the exchange-out kinetics in terms of representing regions of the molecule of differing mobility seems to be not only a reasonable assumption but also the most likely one.

Generally, exchange rates of interior labile protons are evaluated in terms of a structural unfolding model:

$$\mathrm{N(H)} \underset{k_2}{\overset{k_1}{\rightleftharpoons}} \mathrm{O(H)} \xrightarrow{k_3} \mathrm{O(^2H)} \underset{k_2}{\overset{k_1}{\rightleftharpoons}} \mathrm{N(^2H)} \qquad (1)$$

where N indicates the ensemble of "closed" conformers in which the proton considered is not accessible to the deuteriated solvent (e.g., because of internal hydrogen binding), O indicates the open conformation in which the proton is now in contact with the external solvent, k_1 and k_2 are the rate constants for the opening and closing processes, respectively, and k_3 is the intrinsic exchange rate constant for the solvent-accessible proton. Although different limiting kinetic situations may

prevail, studies have shown that exchange of interior backbone amide protons is predominantly via an EX_2 mechanism (Roder et al., 1985). In this limiting situation, the observed exchange rate, k_{ex}, is

$$k_{ex} = (k_1/k_2)k_3 \quad (2)$$

Thus, with a knowledge of the intrinsic rate constant, k_3 [which we have assumed is close to that for the unstructured PDLA molecule taken from O'Neil and Sykes (1988) and calculated according to the equations of Roder et al. (1985)], we can interpret the observed exchange rates of TM in terms of the equilibria between the open and closed conformations of this molecule.

From the observed exchange-out kinetics of TM at low pH, we found that decay parameters fitted best to a three-exponential fit even though the data would fit to four exponentials. The average population sizes of these for gizzard TM are 147, 74, and 61 amide hydrogens (Table I) whose exchange rates are approximatately retarded by factors of 10, 1000, and 100000, respecitvely (Figure 4), at pH 2.0. This immediately implies that regions of greatly varying mobility are present, with over half the molecule being in a mobile conformation.

Although it was not possible to directly measure exchange in the pH range 6–11, the pH dependence of saturation transfer between the amide hydrogen and water does give information on the amide exchange rate at these pH values. Visual inspection of Figure 5 reveals that at pH 6.2 approximately half the number of amides have been lost to saturation transfer, indicating that their exchange rate is very close to that for PDLA, whereas at pH 7.0, 120 amides are present, showing that their exchange rate is slowed about 10-fold relative to PDLA. Of these, about 50 remain at pH 10, therefore demonstrating their rates are some 100000-fold retarded compared to the random-coil structure (a pH shift of 1 pH unit = 10-fold retardation). These observations suggested that we could "model" the results using the parameters derived from the direct exchange experiments but with increased rates to reflect the decreased stability of TM. The dashed line in Figure 5 represents attempt at this; the population sizes are 130 (the model is for nonpolymerizable gizzard TM, and so we have removed 18 residues from this class), 74, and 61 with exchange rates 2-, 10-, and 10^5-fold slower than PDLA. Comparison of the calculated curve for the model TM with the observed results for the gizzard and cardiac TMs shows that although the agreement between these is not perfect, especially in the pH range 6.2–6.6 where the data would indicate that the real structure is more mobile, i.e., closer to the random-coil model, it is a reasonable approximation. Thus, the inference from these results is that at physiological pH as well as low pH, over half the TM molecule is in a highly mobile, loosely structure conformation while about 60 residues are in a more rigid and static environment. This latter region could serve an important role in the folding and stabilization of TM. It is interesting to note that exchange rate at low pH in this region which might be related to the helix to coil transition is of the order of 10^{-5} per minute which is comparable to the value of 10^{-4} per minute reported for the central region of poly(L-glutamic acid) at pH 4.5 (Nakanishi et al., 1972). Also, in the only other report on the exchange characteristics of the amide hydrogens of TM (Hartshorne & Stracher, 1965) a group of about 45 amides were found to exchange slowly at pH 6.0, and presumably these correspond to the most stable set of amides identified in the present report.

We have thus observed that at both low pH and physiological pH, over half of the backbone amide protons of TM have a retardation factor for exchange of less than 10. This value is less than the values found for helical segments of globular proteins such as apamin, BPTI, and RNase which have retardation factors of approximately 10^2, 10^3, and 10^4, respectively. Thus, while the two helices of TM are coiled around one another, protons in these helices do not have the same protection from exchange as helices more buried in globular proteins.

The idea that over half of the TM molecule is very loosely structure is not new. Studies on the conformational stability of rabbit skeletal TM to thermal denaturation (Woods, 1976, 1977; Williams & Swenson, 1981; Potekhin & Privalov, 1982; Betteridge & Lehrer, 1983) have indicated that the C-terminal half of the molecule is more labile than the N-terminal part of the molecule. Also, investigations, carried out in this laboratory, on the variation with temperature of the stabilities and α-helical contents of fragments of rabbit skeletal TM have demonstrated that those from the C-terminal half were of lower stability and α-helical content than the corresponding N-terminal ones (Pato et al., 1981), a conclusion which was further supported by calculations, using the α-helix parameters of Chou and Fasman (1974), on the periodicity of the α-helical potential along the length of the rabbit cardiac TM molecule, which was well developed in the N-terminal half but became prorgressively less so toward the C-terminus (Smillie et al., 1980).

Evidence for the presence of different conformational states in the C-terminal half of striated muscle TM has also come from NMR investigations of striated muscle TMs. Edwards and Sykes (1978, 1980) showed that histidine-153 and -276 NMR resonances at 270 MHz are split due to differences in their local environment producing different pK_a values. Their detailed analysis of this phenomena indicated that each histidine had at least three different conformational states available to them, one of which corresponded to the chain-open or denatured state.

Further support for our model of the structure of TM is provided from the crystal structure of skeletal TM at 15-Å resolution (Phillips et al., 1986). Considerable flexibility could be discerned in the structure especially in the C-terminal half, as judged by the variation in the refined isotropic temperature factors along the length of the molecule. Importantly, these factors increased significantly with temperature for the C-terminal half, indicating that this part of the molecule is extremely mobile at physiological temperatures, whereas the factors for the N-terminal domain stayed relatively constant with temperature.

ACKNOWLEDGMENTS

We thank Professors C. M. Kay and R. McElhaney for the use of their laboratory facilities, Dr. Ruthven Lewis for the differential scanning calorimetry, Vic Ledsham, Mike Nattriss, and Kim Oikawa for sedimentation equilibrium, amino acid, and circular dichroism analyses, respectively. Gerry McQuaid for maintenance of the NMR instrument, and Dawn Oare and Vickie Luxton for preparation of the manuscript. Lastly, Dr. D. J. O'Neil has contributed greatly to this work in the form of both stimulating conversations and suggestions for experimental protocols.

REFERENCES

Adelstein, R. S., & Eisenberg, E. (1980) *Annu. Rev. Biochem. 49*, 921–956.

Betteridge, D. R., & Lehrer, S. S. (1983) *J. Mol. Biol. 167*, 481–496.

Bundi, A., & Wuthrich, K. (1979) *Biopolymers 18*, 285–297.

Chervenka, C. H. (1969) in *A Manual of Methods for the Analytical Ultracentrifuge*, Spinco Division of Beckman

Instruemtns Inc., Palo Alto, CA.
Chou, P. Y., & Fasman, G. D. (1974) *Biochemistry 13*, 211–222.
Côté, G. P. (1983) *Mol. Cell. Biochem. 57*, 127–146.
Edwards, B. F. P., & Sykes, B. D. (1977) in *NMR in Biology* (Dwek, R. A., Campbell, I. D., Richards, R. E., & Williams, R. J. P., Eds.) Academic, New York.
Edwards, B. F. P., & Sykes, B. D. (1978) *Biochemistry 17*, 684–689.
Edwards, B. F. P., & Sykes, B. D. (1980) *Biochemistry 19*, 2577–2583.
Englander, S. W., & Kallenbach, N. R. (1984) *Q. Rev. Biophys. 16*, 521–655.
Hartshorne, D. J., & Stracher, A. (1965) *Biochemistry 4*, 1917–1923.
Hartshorne, D. J., Gorecka, A., & Askoy, M. O. (1977) in *Excitation–Contraction Coupling in Smooth Muscle* (Casteels, R., Godfraind, T., & Ruegg, J. C., Eds.) pp 377–384, Elsevier/North-Holland, Amsterdam.
Heeley, D. H., Golosinska, K., & Smillie, L. B. (1987) *J. Biol. Chem. 262*, 9971–9978.
Helfman, D. M., Feramisco, J. R., Ricci, W. M., & Hughes, S. H. (1984) *J. Biol. Chem. 259*, 14136–14143.
Hill, T. L., Eisenberg, E., & Greene, L. (1980) *Proc. Natl. Acad. Sci. U.S.A. 77*, 3186–3190.
Laiken, S. L., & Printz, M. P. (1970) *Biochemistry 9*, 1547–1553.
Lau, S. Y. M., Sanders, C., & Smillie, L. B. (1986) *J. Biol. Chem. 261*, 7257–7263.
Leavis, P. C., & Gergely, J. (1984) *CRC Crit. Rev. Biochem. 16*, 235–305.
Lehrer, S. S., & Morris, E. P. (1984) *J. Biol. Chem. 259*, 2070–2072.
Lehrer, S. S., Betteridge, D. R., Graceffa, P., Wong, S., & Seidel, J. C. (1984) *Biochemistry 23*, 1591–1595.
MacLeod, A. R. (1987) *BioEssays 6*, 208–212.
Mak, A. S., & Smillie, L. B. (1981) *Biochem. Biophys. Res. Commun. 101*, 108–214.
Nakanishi, M., Tsuboi, M., Ikegami, A., & Kanehisa, M. (1972) *J. Mol. Biol. 64*, 363–378.
O'Neil, J. D. J. & Sykes, B. D. (1988) *Biochemistry 27*, 2753–2762.
Pato, M. D., Mak, A. S., & Smillie, L. B. (1981) *J. Biol. Chem. 256*, 593–601.
Payne, M. R., & Rudnick, S. E. (1985) *Cell Muscle Motil. 6*, 141–184.
Phillips, G. N., Fillers, J. P., & Cohen, C. (1986) *J. Mol. Biol. 192*, 111–131.
Potekhin, S. A., & Privalov, P. L. (1982) *J. Mol. Biol. 159*, 519–535.
Roder, H., Wagner, G., & Wuthrich, K. (1985) *Biochemistry 24*, 7407–7411.
Ruiz-Opazo, N., & Nadal-Ginard, B. (1987) *J. Biol. Chem. 262*, 4755–4765.
Sanders, C., & Smillie, L. B. (1984) *Can. J. Biochem. Cell Biol. 62*, 443–448.
Sanders, C., & Smillie, L. B. (1985) *J. Biol. Chem. 260*, 7264–7275.
Sanders, C., Burtnick, L. D., & Smillie, L. B. (1986) *J. Biol. Chem. 261*, 12774–12778.
Small, J. V., & Sobieszek, A. (1980) *Int. Rev. Cytol. 64*, 241–306.
Smillie, L. B. (1979) *Trends Biochem. Sci. (Pors. Ed.) 4*, 151–154.
Smillie, L. B. (1982) *Methods Enzymol. 85*, 234–241.
Smillie, L. B., Pato, M. D., Pearlstone, J. R., & Mak, A. S. (1980) *J. Mol. Biol. 136*, 199–202.
Sobieszek, A. (1982) *J. Mol. Biol. 157*, 275–286.
Talbot, J. A., & Hodges, R. S. (1982) *Acc. Chem. Res. 15*, 224–230.
Walsh, M. P., Bridenbaugh, R., Kerrick, G. L., & Hartshorne, D. J. (1983) *Fed. Proc., Fed. Am. Soc. Exp. Biol. 42*, 45–50.
Williams, D. L., & Swenson, C. A. (1981) *Biochemistry 20*, 3856–3864.
Williams, D. L., Greene, L. E., & Eisenberg, E. (1984) *Biochemistry 23*, 4150–4155.
Woods, E. F. (1976) *Austr. J. Biol. Sci. 29*, 405–418.
Woods, E. F. (1977) *Austr. J. Biol. Sci. 30*, 527–542.